TECHNICAL MEMORANDUMS
NATIONAL ADVISORY COMMITTEE FOR AERONAUTICS

No. 1050

HEAT TRANSFER OVER THE CIRCUMFERENCE OF A HEATED CYLINDER IN TRANSVERSE FLOW

By Ernst Schmidt and Karl Wenner

Forschung auf dem Gebiete des Ingenieurwesens
Vol. 12, No. 2, March-April 1941

Washington
October 1943

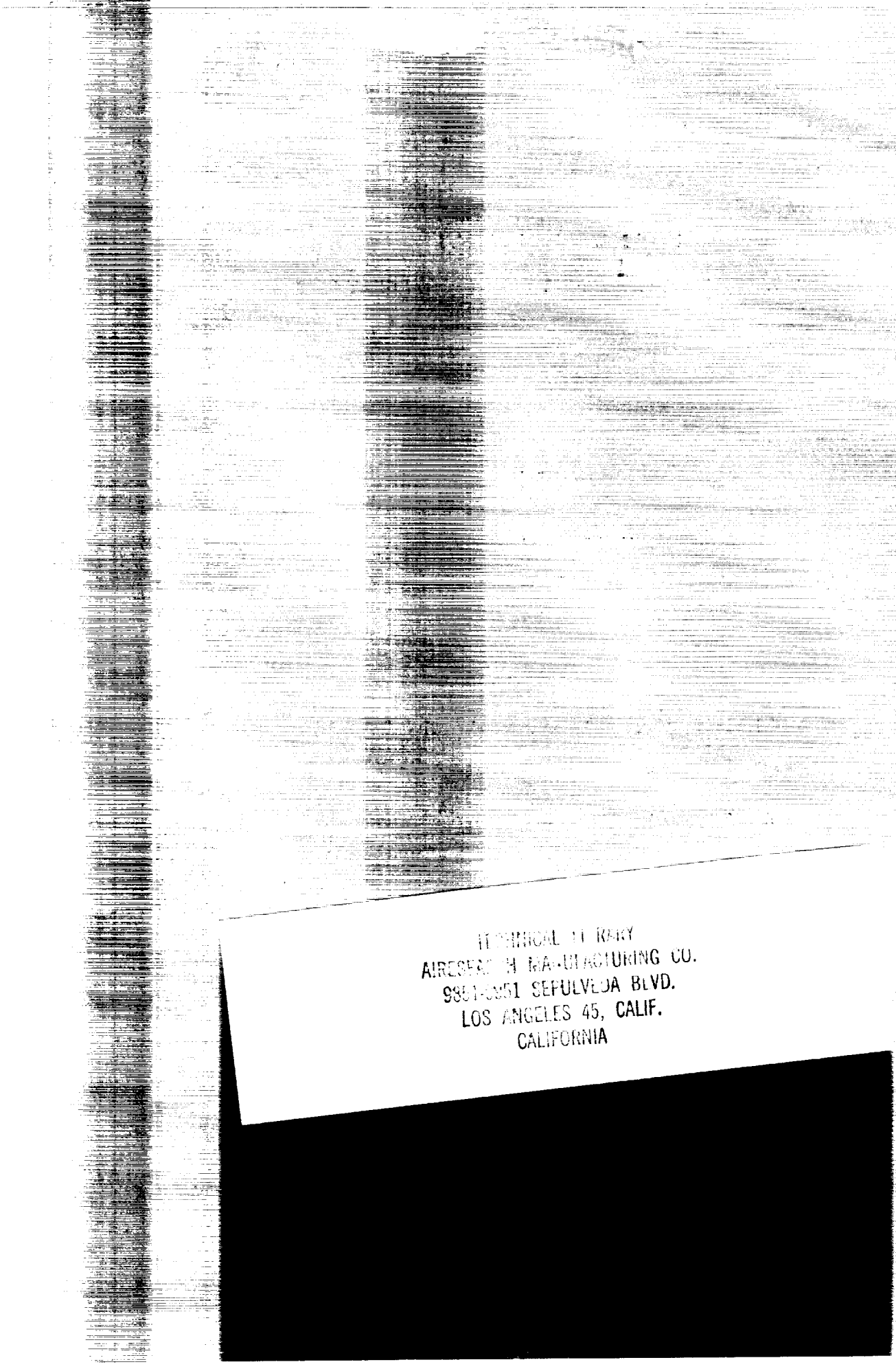

NATIONAL ADVISORY COMMITTEE FOR AERONAUTICS

TECHNICAL MEMORANDUM NO. 1050

HEAT TRANSFER OVER THE CIRCUMFERENCE OF A HEATED CYLINDER IN TRANSVERSE FLOW

By Ernst Schmidt and Karl Wenner

SUMMARY

A method for recording the local heat-transfer coefficients on bodies in flow was developed. The cylinder surface was kept at constant temperature by the condensation of vapor except for a narrow strip which is heated separately to the same temperature by electricity. The heat-transfer coefficient at each point was determined from the electric-heat output and the temperature increase. The distribution of the heat transfer along the circumference of cylinders was recorded over a range of Reynolds numbers of from 5000 to 426,000. The pressure distribution was measured at the same time. At Reynolds numbers up to around 100,000 high maximums of the heat transfer occurred in the forward stagnation point at 0° and on the rear side at 180°, while at around 80° the heat-transfer coefficient on both sides of the cylinder behind the forward stagnation point manifested distinct minimums. Two other maximums occurred at around 115° behind the forward stagnation point between 170,000 and 426,000. At 426,000 the heat transfer at the location of these maximums was almost twice as great as in the forward stagnation point, and the rear half of the cylinder diffused about 60 percent of the entire heat. The tests are compared with the results of other experimental and theoretical investigations.

INTRODUCTION

While the following measurements on the distribution of the heat transfer along the circumference of cylinders had been made by the machine laboratory of the Danzig

---

*"Wärmeabgabe über den Umfang eines angeblasenen geheizten Zylinders." Forschung auf dem Gebiete des Ingenieurwesens, vol. 12, no. 2, March-April 1941, pp. 65-73.

Technical Institute in 1935-36, their publication had been held in abeyance pending their extension to still higher Reynolds numbers. Meanwhile Krujilin (reference 1) in 1938 published similar measurements at about the same Reynolds numbers the results of which are qualitatively in agreement with our own experiments. He too observed at high Reynolds numbers the markedly defined maximum of the heat transfer at 110° to 120° behind the forward stagnation point. But quantitatively there are considerable discrepancies. At Re = 39,500 his reported heat transfer in the forward stagnation point is 30 percent greater than in our tests and at Re = 425,000 it is 35 percent. His values are too high by about the same amounts compared to the measurements of all the other observers whose averages are in good agreement with ours. The calculation of the heat transfer in the forward stagnation point of cylinders by Squire (unpublished but mentioned in "Modern Developments in Fluid Dynamics" vol. 2, Oxford, 1938, p. 631) is also in agreement with our experiments.

TEST METHOD AND EXPERIMENTAL LAYOUT

A fixed wall of area F and temperature t_w transmits by conduction and convection on air with the temperature t_L measured at sufficient distance from the wall in unit time the heat volume

$$Q = \alpha F(t_w - t_L) \tag{1}$$

where

α heat-transfer coefficient

On a cylinder of diameter d heated transversely by air with velocity w the heat-transfer coefficient α depends, besides the Reynolds number $Re = wd/\nu$ of the flow, on the location of the particular area on the cylinder circumference.

Introducing the heat-transfer coefficient in nondimensional form as Nusselt number $Nu = \alpha d/\lambda$, where λ is the thermal conductance of air, it affords a relation of the form

$$Nu = f(Re,\varphi) \qquad (2)$$

if φ is the angle counted from the forward stagnation point characterizing the position of the heat-diffusing surface particle on the tube circumference.

Neither the shape nor the temperature of the cylinder surface must be subjected to a perceptible variation during the measurement of the local heat diffusion, so as not to disturb the field of velocity and temperature. The following method was therefore employed: The major portion of the heat-diffusing surface of the hollow brass cylinders was kept at a constant temperature of 100° by internal heating with vapor of atmospheric pressure, except at one place (fig. 1), where a strip of the surface was removed and replaced by a thick, hollow copper bar heated internally by electricity. This heating element was insulated by an air layer bounded by polished metal surfaces. The surfaces of the heating element and vapor-heated cylinder meet at the cylinder circumference to within a clearance of about 0.3 millimeter in width, which is coated with bakelite lacquer so that no interruption of the smooth cylindrical surface occurs.

Figure 2 is a perspective sectional view of the design; a is the heating element in form of a hollow, rectangular copper bar, housing the heating coil b. The thermocouples c soldered to the heating element pass through pipe d to the outside. The heating element is so supported in box e by means of the pertinax straps f as to leave between both an isolating air space bounded by polished metal surfaces. The surface temperature of the vapor-heated cylinder part is measured at four points g in tubing h along the circumference, soldered from the inside to the cylinder wall. The tubing h passes through the vapor chamber to a hole in the cylinder by means of which the pressure distribution along the circumference can be determined. The vapor for heating the cylinder is fed through tube i in such amounts that always an excess flows off through pipe k into a condensator to prevent air from entering the vapor chamber.

The electric heating of the copper bar is so adjusted that it assumes the same temperature as the vapor-heated cylinder portion. The temperatures were recorded with soft-soldered manganin-constantan thermocouples of 0.3 millimeter in diameter by means of a Wolff compensator according to Diesselhorst. Four to six thermocouples

each were employed on both the copper bar and the cylinder. Originally all temperatures were measured against one cold junction, but later on only the difference between the cylinder and the copper bar was determined for simplicity, where, in view of the small difference in this range the calibration curve of the thermocouples could be regarded as a straight line with a slope 0.02126° C at 0.001 millivolt. The air temperature was measured by a heat-resistant thermometer inserted laterally in the jet; it ranged between 20° and 26° C in the different tests and in one test was constant to 0.1°.

The heating element can be turned as indicated in figure 1 through any desired angle φ in respect to the flow direction by turning the whole tube about its axis and a graduated disk. By turning the tube the pressure test station of tubing h is moved with it and supplies the pressure distribution p over the circumference. The output of the heating element ascertained with precision ammeter and voltmeter gives the heat transfer of the part of the cylinder surface occupied by it. Half the area of the small gap filled with bakelite between heating element and cylinder is counted as heating surface.

The cylinder with the heating element was mounted upright in the air stream of a rectangular nozzle of 300 millimeters in width and 250 millimeters in height, and placed in the partition wall of two rooms of 6 by 5 and 6 by 4 square meters floor space and 3 meters in height. A Betz ventilator with diffuser in a second opening of the same wall pushed the air from the larger into the smaller room from which it was returned through the nozzle into the first. Stilling surfaces assured disturbance-free air flow into the nozzle. In an earlier study with the same nozzle arrangement Hilpert (reference 2) proved that the employed nozzle gives an air stream of very uniform velocity distribution. The flow velocity could be varied between 2 and 33 meters per second by means of the ventilator. To assure a fairly constant air stream with respect to time, the ventilator was driven from two separate storage batteries, one feeding the field, the other the armature. By adding an appropriate number of cells to the armature battery the rotational speed in the armature circuit could be varied within wide limits without variable rheostat and kept very constant.

The airspeed was determined from the pressure difference of the two rooms before and behind the nozzle and also with a Prandtl pitot tube.

The pressure distribution on the cylinder circumference was determined by the cited orifice of 1 millimeter, the static pressure p_o in undisturbed flow and the equivalent pressure of the test chamber, respectively, into which the jet entered, serving as reference pressure. The pressures were recorded with a micromanometer filled with xylol, calibrated by means of a Levy-type pressure balance (reference 3), and supplemented at high pressures by an Askania water-column minimeter.

EXPERIMENTAL CYLINDERS

The cylinders were 50, 100, and 250 millimeters in diameter. The dimensions of the heating elements are appended in table I. The 50-millimeter cylinder was fitted in the nozzle with its axis parallel to the 600-millimeter long nozzle edge; but in one test with Re = 8290 it stood upright, that is, parallel to the short edge of the nozzle.

End disks of 250-millimeter diameter inserted perpendicular to the axis on the cylinder removed the disturbing effect of the cylinder ends on the flow. The 100- and the 250-millimeter cylinder were mounted with their axis at right angles to the longitudinal edges of the nozzle. The 600-millimeter long exit edges of the nozzle were lengthened by flat plates of cardboard through which the ends extended into the test cylinder. The distance from cylinder axis to nozzle-exit opening amounted to 165 millimeters on the 50-millimeter cylinder and to 360 millimeters on the two others. Figure 3 is a photograph of the setup showing the nozzle a and the 100-millimeter cylinder b. Directly below, the electrically heated boiler for producing the vapor is indicated as thick cylinder c wrapped in aluminum foil.

An estimate of the effect of the end disks perpendicular to the axis of the tube on the basis of the Blasius equation for laminar-boundary-layer thickness on a flat plate gave at the lowest airspeed a thickness of 0.75 centimeter. Since the ends of the heating elements were always about 50 millimeters from the end disks, its effect does not extend as far as the heating element.

TESTING PROCEDURE AND EVALUATION

After an initial run of the motor and after the air stream had become constant with respect to time, the heat output of the copper bar was regulated so that its temperature in the steady state was the same as that of the vapor-heated portion of the cylinder surface. To save time, small but constant temperature variations up to $\pm 0.4^\circ$ were at times tolerated during the adjustment. The small thermal interchange Q_l involved between heating bar and vapor-heated surface was obtained by special calibration tests and applied as correction.

The amount of heat diffused by radiation

$$Q_s = \epsilon C_s F[(T_w/100)^4 - (T_L/100)^4]$$

must be deducted from the electrically measured heat output Q_g.

F radiating surface, that is, the heat-diffusing surface of the copper bar inclusive of half the bakelite-coated clearance space in square meters

$C_s = 4.96$ kilocalories per square meter per hour (deg K)^4, the radiation factor of the absolutely black body

ϵ emission ratio of the polished copper surface, which with consideration of the more radiating half of the clearance space was appraised at 0.10

$T_w = 273^\circ + 100^\circ$, temperature at the surface

$T_L = 273^\circ + 24^\circ$, surrounding temperature

Table II contains the effective quantities of the radiating surfaces of the heating bars and the values of the radiation-diffused heat quantities Q_s for the different tubes.

Allowance for the corrections Q_l and Q_s, the absolute values of which range at small Re between 0 and 4 percent, at large Re between 0 and 3 percent of the heating performance, affords the heat transfer $q = Q_g - Q_l - Q_s$ of the heating element and thus the heat-transfer coefficient according to equation (1).

The airspeed follows from $w = \sqrt{2g\ \Delta P/\gamma}$, where ΔP (kg/m^2) is the pressure difference between pressure and suction space before and behind the nozzle, g = 9.81 meters per second per second, the gravitational acceleration, and γ (kg/m^3) the specific gravity of air. In table III the individual values of the readings and the results computed therefrom are given for a test on the 100-millimeter cylinder at Re = 39,800. ($p-p_o$ is difference of pressure p at location φ of the tube circumference and of the static pressure p_o in undisturbed air stream.)

The principal data of the tests are collected in table IV. The calculation of Nu and Re was based on the planimetered average values of λ = 0.0241 kilocalories per meter per hour per degree Centigrade and $\nu = 19.4 \times 10^{-6}$ square meters per second between 24° and 100° C.

RESULTS OF TESTS

In figures 4 to 6 the dimensionless Nu obtained from the experiments are shown plotted against the angle φ for different Re. Starting from the stagnation point the heat-transfer coefficient drops to a distinct minimum close before $\varphi = 90°$ and then rises again, which is so to much higher values as Re is greater.

It is to be noted that the test points give the local average value of α over the width of the heating bar. Hence at places where the heat-transfer coefficients plotted against φ have a minimum, the curve of the local heat-transfer coefficient must extend below the measured values and vice versa.

The peculiar distribution is even plainer in the polar diagrams of figure 7. At around $\varphi = \pm 115°$ distinct maximums of the heat transfer occur for Reynolds numbers above 200,000, and which at Re = 426,000 are almost twice as high as in the stagnation point. On the rear of the cylinder at $\varphi = 180°$ the heat-transfer coefficients for Reynolds numbers of from 25,000 to 426,000 are greater than in the forward stagnation point.

These phenomena were not known at the time of our experiments, since measurements of this nature at such large Reynolds numbers were up to then unavailable, although Krujilin had published similar results in 1938 (reference 1).

In general, the measurements were limited to half the cylinder circumference; but as a check on the symmetry several check measurements of the heat transfer and the pressure distribution were carried out over the entire circumference without, however, manifesting any substantial differences between both halves.

The pressure distribution at different Re measured on the heated tube is given in figure 8. The minimum of the pressure distribution lies before the minimum of the heat-transfer coefficient indicated with α_{min}. At Re between 180,000 and 400,000, that is, in the so-called critical-resistance region in which the marked drop of the resistance coefficient occurs, the known strong pressure minimum is seen at φ closely below 90°. The very small low pressure at the back is probably attributable to the insufficient width of the jet compared to tube diameter. The jet is to some extent split by the cylinder.

Interesting parallels are obtained when the distribution of the heat-transfer coefficient is compared with measurements of the shear-stress distribution on the wall of a circular cylinder as made by Fage and Falkner (reference 4) with a Stanton-type exploring tube. Besides the heat-transfer distribution together with the corresponding pressure distribution by our measurements at Re = 426,000, that is, in the post-critical region, figure 9 shows a shear-stress distribution by Fage and Falkner at Re = 188,000, but with turbulence grid in the flow before the test cylinder. The peculiarity of the shear-stress curve indicates that through the turbulence grid a critical or post-critical flow form has been attained even at the still comparatively small Reynolds number. For the rest the curve is less interesting quantitatively than qualitatively.

The minimum of the heat-transfer coefficient agrees with the minimum of the frictional intensity which according to Fage and Falkner is also indicated in the pressure-distribution curve by an inflection point. Near this

inflection, they concluded, a transition from laminar to turbulent flow takes place in the boundary layer. The observed second maximum of the heat-transfer coefficient, at around $\varphi = 115^{\circ}$, appears too in the shear-stress-distribution curve as second maximum. Obviously the cause of both effects is a common one: Through the turbulent interchange of momentum the boundary layer behind the place of the minimum is newly accelerated. Not until the second maximum has been reached does the orderly boundary-layer flow cease and the boundary layer separate from the flow.

COMPARISON WITH OTHER DATA

Various measurements of other observers on the distribution of the heat transfer at $Re = 39,600$ are compared in figure 10 with the data of the present report at $Re = 39,800$, that is, practically for the same Reynolds number.

In closest agreement with our experiments are the measurements of Small (reference 5) who measured the temperature gradient in a layer of a poor heat conductor inserted as sector in the tube with a thermopile. But the peak of his curve at $\varphi = 0$ is most unlikely. His measurements do not go to such high Reynolds numbers as ours. The experiments of Drew and Ryan (reference 6) and of Klein (reference 7) are less reliable. The test method of Lohrisch (reference 8) who inferred the heat transfer from the absorption of ammonium is afflicted with even greater sources of error. Krujilin's curve (reference 1) lies considerably above all others. The cause of these departures is likely to be found in the roughness of his tubes of porcelain and cast iron, although in the face of meagerness of data of this report it can only be surmised.

Plotted against the Reynolds number, figure 11 shows the percent of heat transfer apportioned to the back of the tube. At $Re = 5000$ this share amounts to only 30 percent, at $Re = 54,000$ to 50 percent, and at still higher Reynolds numbers it rises to around 60 percent. Even in the critical range of Reynolds number where the resistance of the tube is considerably lower as a result of the reduction of the negative pressure at the back, the proportion of the back to the heat transmission remains large.

The measured distribution curves give, when planimetered, the average heat-transfer coefficients of the entire tube. On comparing the so-obtained values with Hilpert's carefully executed experiments (reference 2) they are found to lie a little above at Reynolds numbers of less than 10^5. These differences are attributable to the inevitably greater measuring errors associated with our method. Possibly the joint between copper bar and tube, in spite of being carefully coated, introduced a small disturbance of the flow and hence a slight increase in heat transfer.

Squire theoretically computed the heat-transfer coefficient in the forward stagnation point of a cylinder and arrived at the formula $Nu = 1.01\sqrt{Re}$. A comparison of his result (straight line) with our measurements is given in figure 13. The agreement is exceptionally good.

INCREASE OF HEAT TRANSFER THROUGH INCREASING TURBULENCE OF FLOW

Prandtl's observations of the effect of a disturbance of flow at the front by an "interference wire" on the resistance of spheres suggested the use of such wires here also.

Figure 14 shows the variation of the heat transfer caused by two straight brass wires 1.5 millimeters in diameter fitted on both sides of the stagnation point at $\varphi = \pm 77.5^\circ$. The heat diffusion is reduced at the front but raised on the back. At the location of the wire a steep jag occurs which in part is due to the greater turbulence and in part to the cooling-fin action of the good heat-conducting quality of the wire. One interesting feature of the curves is that at $\varphi = \pm 115^\circ$ the local maximum is already indicated, which at higher Reynolds numbers occurs at this place as a result of boundary-layer turbulence. The increase at the back exceeds the decrease at the front so that on the whole the interference wire increases the heat transfer. Figure 15 shows the effect of the interference wire on the pressure distribution. Planimetry of the curves with consideration of the direction of the force at the surface of the tube results, of course, in an increase of the resistance of the tube

through the interference wire in contrast to Prandtl tests on spheres. So far these experiments have not been extended to a sufficient range of Reynolds numbers; or else heat-transfer distributions would have been presumably reached at relatively low Reynolds numbers as they occur at the smooth pipe only at high Reynolds numbers.

HEAT TRANSFER AT THE FRONT OF FLOW PROFILES

In order to secure some reference data on the heat transfer at the front of stream profiles with the existing test setup the 100-millimeter cylinder was faired at the back as illustrated in figure 16. The parallel arcs touch with their apex the tube at $\varphi = \pm 90^{\circ}$. This appendage modifies the heat transfer at the front very little; it drops a little at the stagnation point, but for 45° to about 85°, it is most likely increased as a result of the facilitated flowoff.

Translation by J. Vanier,
National Advisory Committee
for Aeronautics.

REFERENCES

1. Krujilin,G.: Technical Physics of the USSR, vol. 5, no. 4, 1938, p. 289.

2. Hilpert, R.: Forsch. Ing.-Wes. Bd. 4, 1933, pp. 215-24.

3. Levy, Fr.: Z. Instrumentenkde. Bd. 45, 1925, pp. 515-21.

4. Fage, A., and Falkner, V. M.: Further Experiments on the Flow around a Circular Cylinder. R. & M. No. 1369, British A.R.C., 1931.

5. Small, J.: Philosophical Magazine. ser. 7, vol. 49, 1935, p. 251.

6. Drew, T. B., and Ryan, W. P.: Trans. Am. Inst. Chem. Engrs. vol. 26, 1931, pp. 118-49.

7. Klein, V.: Diss. T. H. Hannover. 1933.

8. Lohrisch, W.: VDI-Forsch. Heft 322, (Berlin), 1929.

TABLE I

DIMENSIONS OF HEATING ELEMENTS

Number	Cylinder diameter (mm)	Width (mm)	Width (deg)	Length (mm)
1	50	4.7	10.8	200
2	100	12.5	14.3	160
3	250	12.5	5.8	160

TABLE II

HEAT RADIATION

Cylinder diameter (mm)	Heating bar surface (cm^2)	Heat radiation (kcal/hr)
50	9.5	0.050
100	20.1	.115
250	20.1	.115

TABLE III

SINGLE TEST SERIES
[Cylinder d = 100 mm]

Time	Angle φ (deg)	Pressure gradient ΔP (kg/m^2)	Pressure at $180^\circ-\varphi$ $p-p_o$ (kg/m^2)	Air temperature t_L (deg C)	Temperature increase Δt (deg C)	Total heat output Q_g (kcal/hr)	Correction for conduction Q_l (kcal/hr)	Correction for radiation Q_s (kcal/hr)	Heat output Q (kcal/hr)	Temperature difference $t_w - t_L$ (deg C)	Heat transfer coefficient α ($\frac{kcal}{m^2 hr\,^\circ C}$)	Nu number
22.40	0	3.62	-2.98	20.3	-0.06	7.610	0.025	-0.115	7.520	79.5	47.1	195
22.55	20	3.62	-3.06	20.3	-.38	7.360	.155	-.115	7.400	79.3	46.4	193
23.20	40	3.62	-2.82	20.6	.23	6.940	-.095	-.115	6.740	79.5	42.2	175
23.26	60	----	-2.69	20.6	.15	5.575	-.065	-.115	5.395	79.4	33.8	140
24.10	70	3.62	-2.66	20.7	.06	4.100	-.025	-.115	3.960	79.2	24.9	103
.42	80	3.62	-2.66	20.7	.11	2.160	-.045	-.115	2.000	79.2	12.6	52.1
1.20	85	3.62	-2.61	20.7	.06	2.120	-.025	-.115	1.980	79.2	12.4	51.6
1.30	90	----	-2.69	20.7	-.19	2.530	.080	-.115	2.495	78.9	15.7	65.3
2.06	100	3.62	-2.90	20.7	0	3.420	0	-.115	3.305	79.1	20.8	86.1
-----	110	3.62	-3.11	----	----	-----	-----	-----	-----	----	----	-----
2.25	120	3.62	-2.71	20.7	.26	4.255	-.105	-.115	4.035	79.4	25.3	105
3.15	140	----	-0.21	20.6	-.09	5.380	.035	-.115	5.300	79.1	33.3	139
3.30	160	3.62	2.53	20.6	-.43	6.690	.175	-.115	6.750	78.8	42.7	177
4.00	170	3.62	3.41	20.6	.17	7.685	-.070	-.115	7.500	79.4	47.0	195
4.10	180	3.62	3.61	20.6	-.06	7.825	.025	-.115	7.735	79.2	48.7	202

Average values:

b = 755.4 mm Hg, barometric pressure

ΔP = 3.62 kg/m^2, pressure difference, pressure suction space ($\Delta P = 1/2 \rho w_o^2$)

w = 7.73 m/sec, airspeed

t_z = 99.83° C, cylinder temperature (vapor temperature)

Re = 39,800

Nu = 141

λ = 0.0241 kcal/hr $m^\circ C$, thermal conductance of air between 24° and 100° C

ν = 19.4 x 10^{-6} m^2/sec, kinematic viscosity of air between 24° and 100° C

TABLE IV

PRINCIPAL TESTS

Test cylinder d (mm)	Barometric pressure b (mm Hg)	Specific weight of air γ (kg/m^3)	Air-speed w (m/sec)	Reynolds number Re	Nusselt number: Front Nu_V	Nusselt number: Back Nu_R	Nusselt number: Average Nu	Average heat transfer coefficient α $\left(\frac{kcal}{m^2 hr\,^\circ C}\right)$
50	741	1.158	8.23	21,200	111	77	94	45.3
	729	1.146	13.2	33,920	136	117	126	61
	744	1.156	20.5	52,800	174	171	173	83
	760	1.183	3.22	8,290	71	32.1	51.4	24.7
100	757	1.174	33.0	170,000	342	425	384	93
	755	1.189	7.73	39,800	146	134	141	33.8
	756	1.189	12.5	64,450	199	193	196	47.2
	760	1.184	3.02	15,550	91	60	76	18.2
	761	1.186	19.7	101,300	246	283	264	64
250	747	1.171	3.04	39,200	139	97	118	11.8
	747	1.170	7.91	102,000	246	220	233	22.5
	741	1.153	20.0	257,600	412	531	472	45.6
	748	1.167	33.1	426,000	596	826	711	68

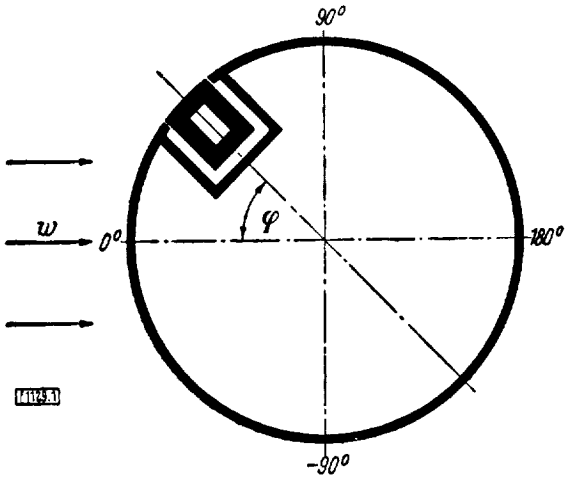

Figure 1.- Section through test cylinder with heating element.

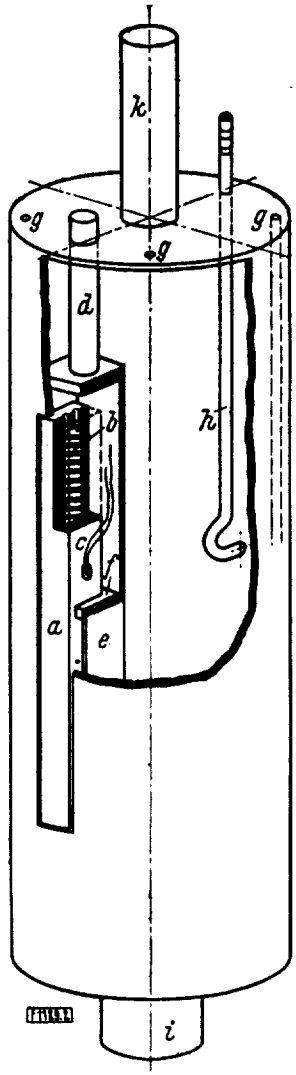

Figure 2.- Test cylinder. a - heating element, b - heating coil, c - thermocouples, d - pipe through which the thermocouples pass, e - box, f - pertinax insulating straps, g - tubing for measuring circumferential temperature, h - tubing for measuring pressure, i - vapor feed pipe, k - vapor discharge pipe.

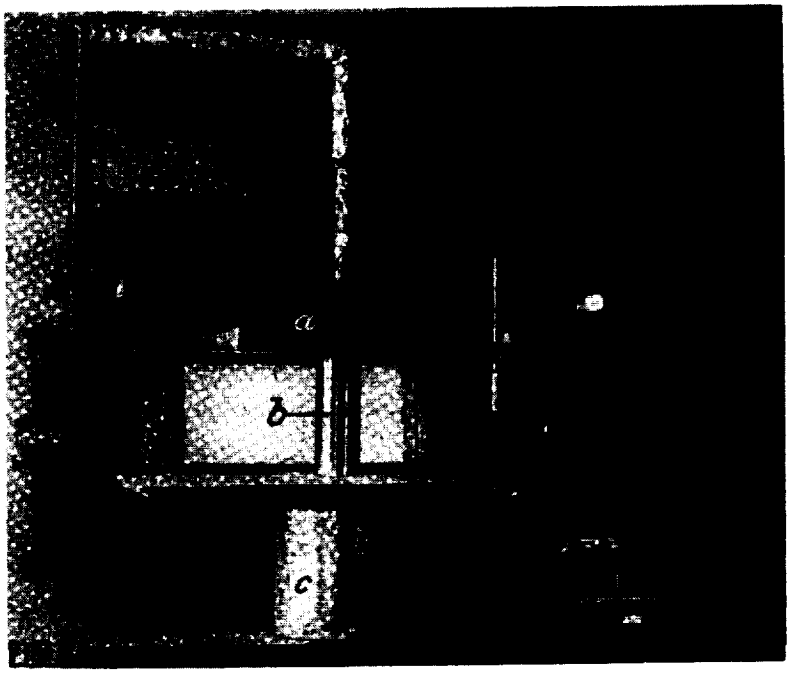

Figure 3.- Experimental set-up. a - rectangular nozzle, b - test cylinder, c - steam boiler.

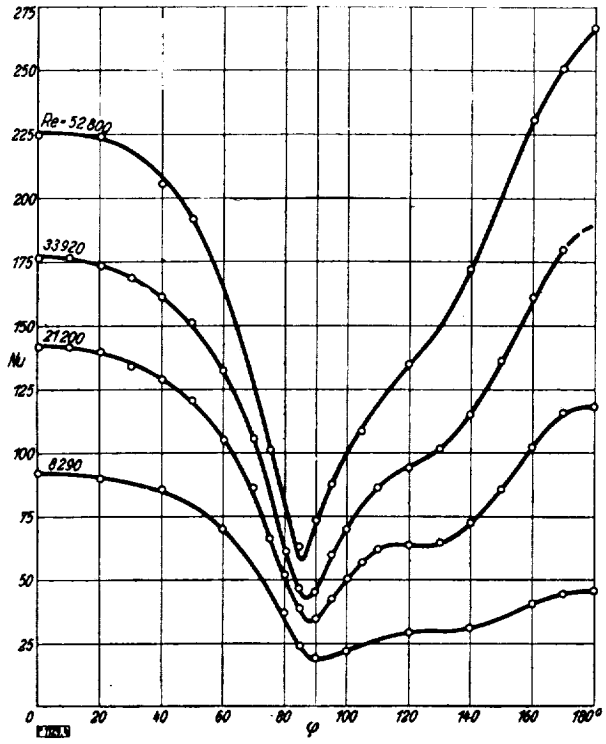

Figure 4.- Heat transfer distributions across the cylinder circumference for different Reynolds numbers. d = mm; α = 0.43 Nu.

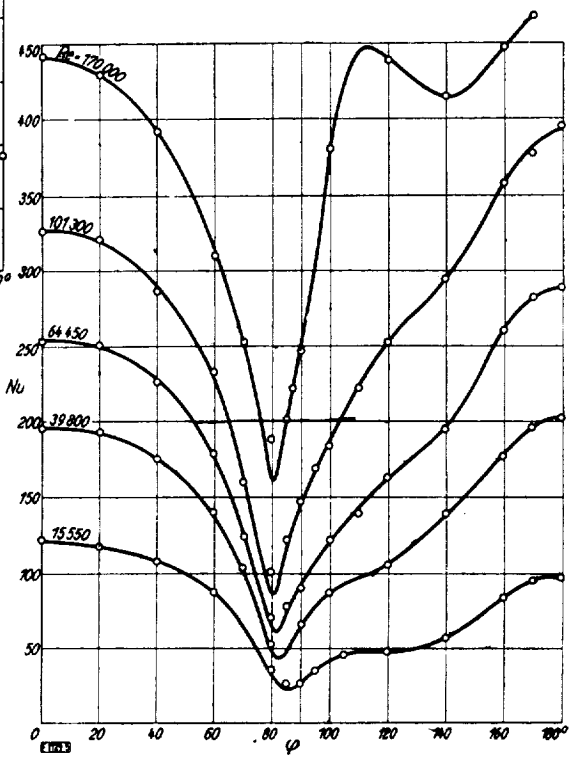

Figure 5.- Heat transfer distribution across the cylinder circumference for different Reynolds numbers. d = 100 mm; α = 0.24 Nu.

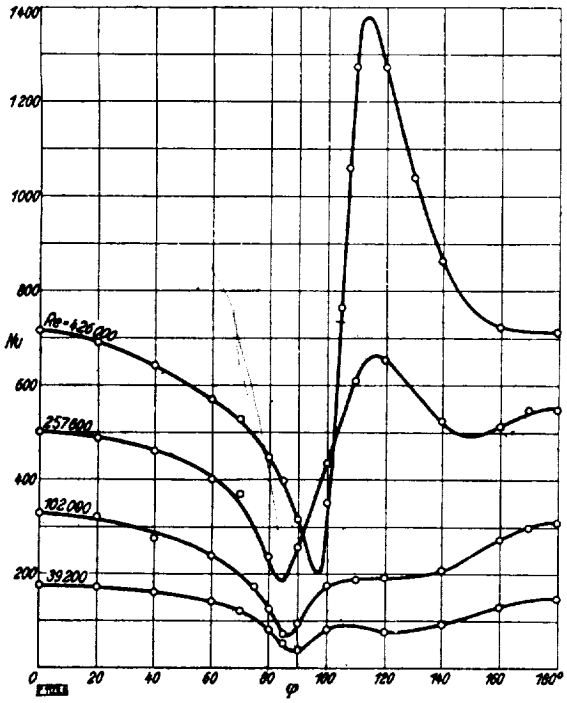

Figure 6.- Heat transfer distribution across the cylinder circumference for different Reynolds numbers. d = 250 mm; α = .097 Nu.

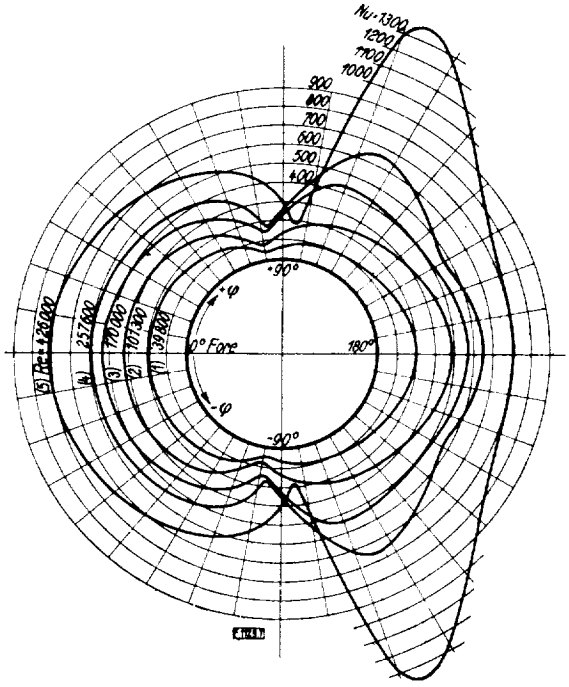

Figure 7.- Typical heat transfer distribution curves in the polar diagram. Curves (1) and (2) in the pre-critical resistance zone, curves (3) and (4) in the critical resistance zone, curve (5) in the post-critical resistance zone, (in a given case, end of critical range). The curves are recorded on one side and symmetrically transferred to the other side.

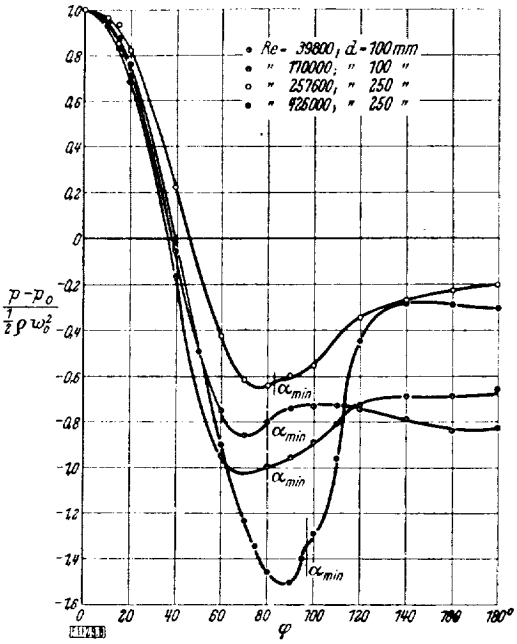

Figure 8.- Pressure distribution curves for different Reynolds nymbers. $p - p_o$ = increment of pressure at tube surface over static pressure p_o in undisturbed flow with velocity w_o and density ρ.

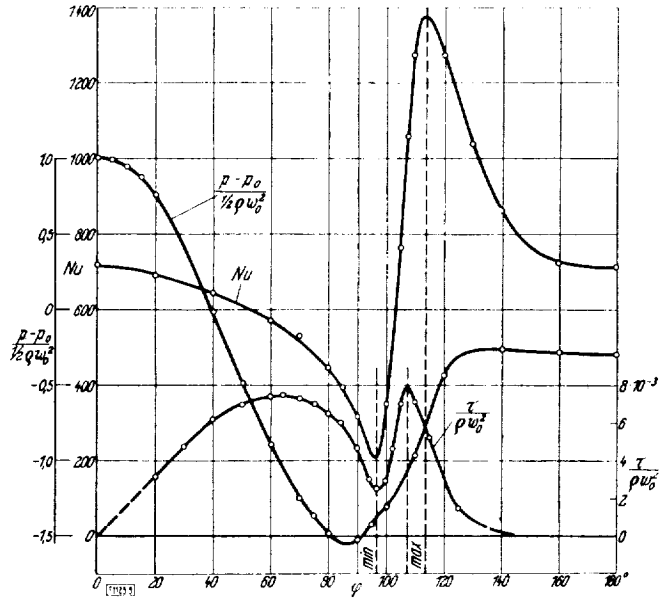

Figure 9.- Distribution of Nusselt number Nu and pressure $\frac{p - p_o}{1/2\rho w_o^2}$ at Re = 426,000 and distribution of skin friction $\frac{\tau}{\rho w_o^2}$ at Re = 168,000 with turbulence grid (according to Fage and Falkner) over the circumference of a cylinder.

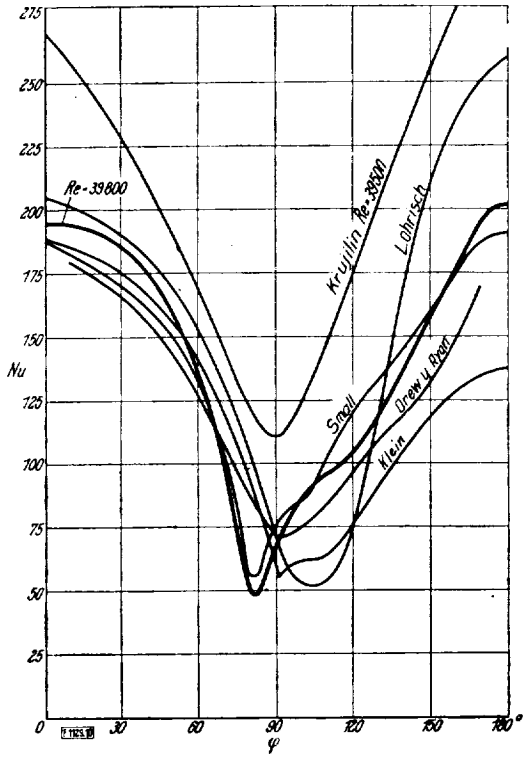

Figure 10.- Comparison of test data for Re = 39,800 with other observers.

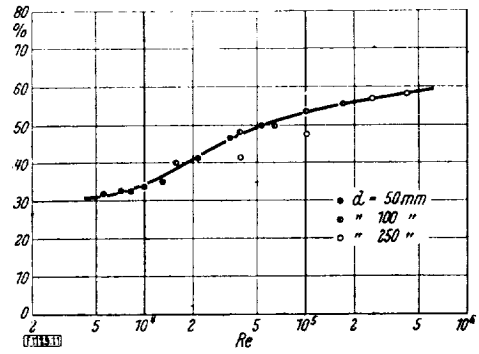

Figure 11.- Proportion of back to the total heat transfer.

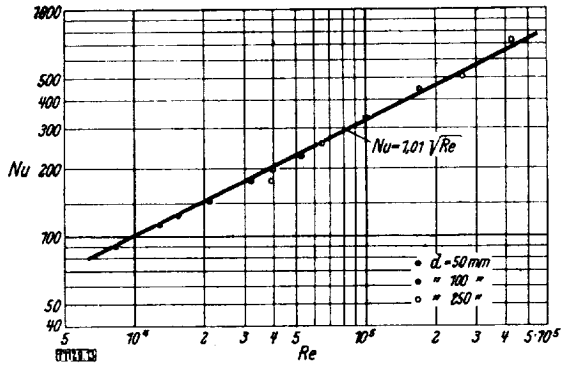

Figure 13.- Heat transfer coefficient in the forward stagnation point of the cylinder. (Solid line represents Squire's theoretical solution.)

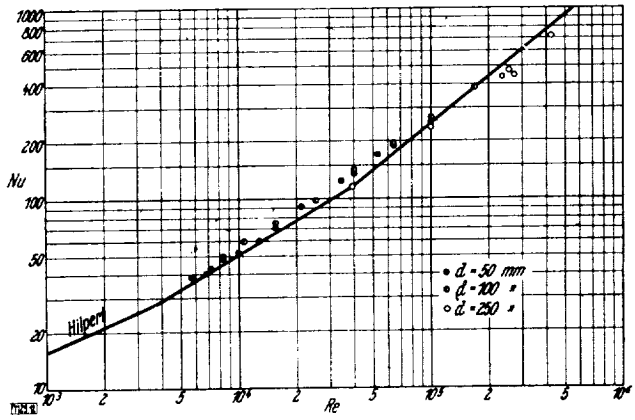

Figure 12.- Comparison of the average heat transfer coefficient for the total cylinder circumference with Hilpert's curve.

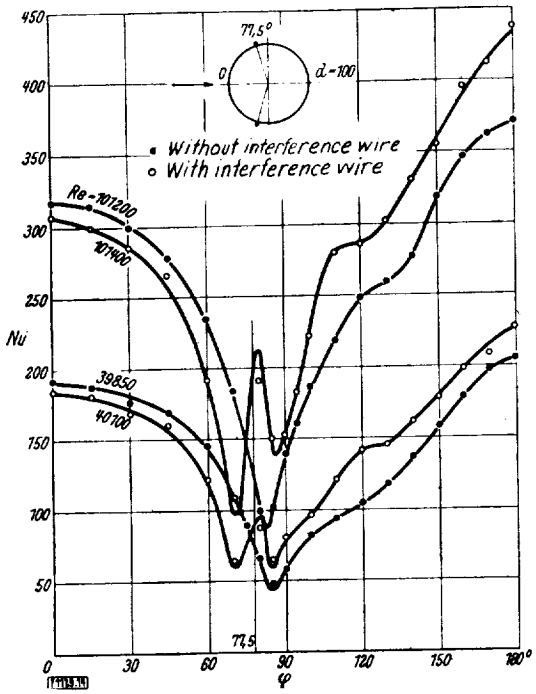

Figure 14.- Effect of interference wire at $\varphi = 77.5^{\circ}$ on heat transfer.

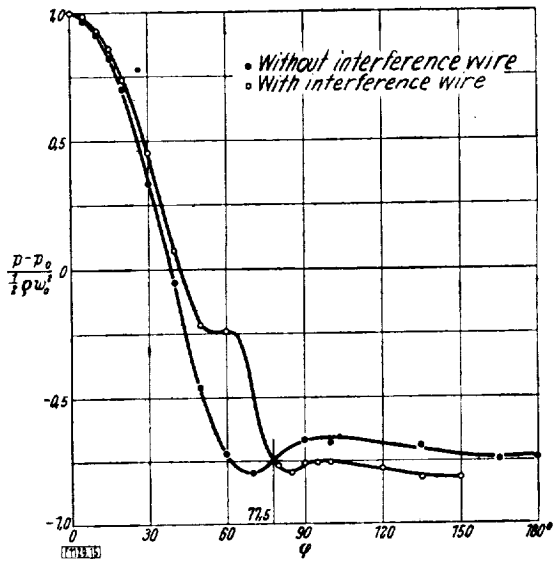

Figure 15.- Effect of interference wire on pressure distribution.

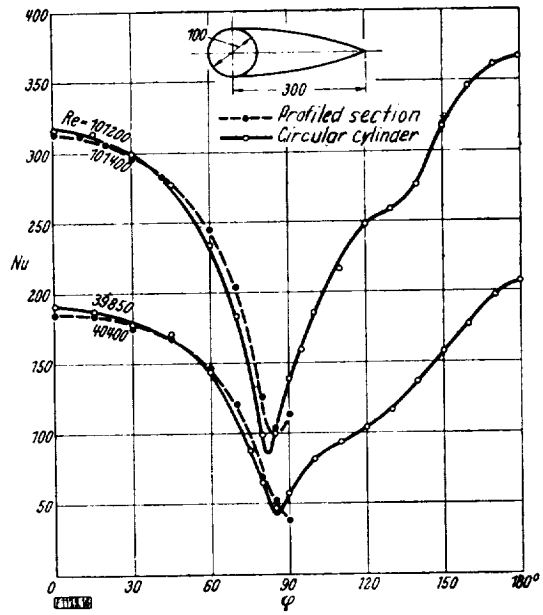

Figure 16.- Effect of fairing at back on heat transfer at front of cylinder.